

Estimating Heterogeneous Survival Treatment Effect via Machine/Deep Learning Methods in Observational Studies

Liangyuan Hu¹, Jiayi Ji¹, Fan Li²

¹Department of Population Health Science and Policy, Icahn School of Medicine at Mount Sinai, New York, NY, USA

²Department of Biostatistics, Yale University, New Haven, Connecticut, USA

Abstract

The rise of personalized medicine necessitates improved causal inference methods for detecting treatment effect heterogeneity (TEH). Approaches for estimating TEH with observational data have largely focused on continuous outcomes. Methods for estimating TEH with right-censored survival outcomes are relatively limited and have been less vetted. Using flexible machine/deep learning (ML/DL) methods within the counterfactual framework is a promising approach to address challenges due to complex individual characteristics, to which treatments need to be tailored. We contribute a series of simulations representing a variety of confounded heterogeneous survival treatment effect settings with varying degrees of covariate overlap, and compare the operating characteristics of three state-of-the-art survival ML/DL methods for the estimation of TEH. Our results show that the nonparametric Bayesian Additive Regression Trees within the framework of accelerated failure time model (AFT-BART-NP) consistently has the best performance, in terms of both bias and root-mean-squared-error. Additionally, AFT-BART-NP could provide nominal confidence interval coverage when covariate overlap is moderate or strong. Under lack of overlap where accurate estimation of the average causal effect is generally

challenging, AFT-BART-NP still provides valid point and interval estimates for the treatment effect among units near the centroid of the propensity score distribution.

Keywords: Causal inference; Bayesian Additive Regression Trees; Treatment effect heterogeneity; Machine/Deep learning; Individual survival treatment effect; Observational studies.

Although traditional methods for observational studies focus on estimating the average effect among a target population, the rise of personalized medicine and the increasing complexity of comparative effectiveness study have generated a more patient-centric view for drawing inference with biomedical and epidemiologic data. As a result, treatments need to be tailored to the covariate distribution of the target population, which necessitates the evaluation of treatment effect heterogeneity (TEH). If TEH exists, there is an underlying partition of the population into subgroups across which the treatment effect differs. Because the assessment of TEH requires addressing challenges due to complex and oftentimes high-dimensional individual characteristics, using flexible modeling techniques such as machine learning methods within the counterfactual framework has gained traction. For example, Foster et al. (1) study the virtual twins approach that first uses random forests (RF) to estimate the *individual treatment effect* (ITE) by differencing predicted counterfactual outcomes under treatment and under control for each unit, and then regresses the predicted ITEs on covariates to identify subgroups with a treatment effect that is considerably different than the average treatment effect (ATE). Wager and Athey (2) develop the causal forests for ITE estimation. Lu et al. (3) compare several RF methods, including RF and causal forests, for predicting ITE and found that the synthetic RF had

the best performance. Hill (4) adapts Bayesian Additive Regression Trees (BART) into causal inference and describes visualization of the modes of the predicted ITEs for hints about the underlying number of subgroups. Anoke et al. (5) *a priori* set the number of subgroups and group observations based on percentiles of the empirical distribution of either the ITEs or propensity scores (PS) and estimate a treatment effect within each subgroup. They compare several modern machine learning (ML) methods including BART, gradient boosted models (GBM) and the facilitating score (FS) to estimate TEH and find BART performs the best in their simulation studies.

Despite these previous studies, methods for estimating TEH in observational studies with right-censored survival outcomes have not received much attention, with the following exceptions. Henderson et al. (6) develop a nonparametric accelerated failure time (AFT) model using BART to flexibly capture the relationship between covariates and the failure times for the estimation of ITE. Tian et al. (7) approach the problem of the TEH estimation by modeling interactions between a treatment and a large number of covariates. Both methods are designed for analyzing data from randomized clinical trials. Shen et al. (8) use RF with weighted bootstrap to estimate the optimal personalized treatment strategy, but the estimation of TEH is not the focus of their paper. Cui et al. (9) extend the causal forests of Wager and Athey (2) for ITE estimation to accommodate censored survival data, and use bootstrap for inference. Tabib and Larocque (10) propose a new RF splitting rule to partition the survival data with the goal of maximizing the heterogeneity of the ITE estimates in the left and right nodes from a split. Neither of the last two works has made software available at this time.

Survival outcome is typically the primary outcome in cancer epidemiology studies. As an example, a recent study shows that brachytherapy-based radiotherapy leads to similar long-term survival probability on the population level as radical prostatectomy for treating high-risk localized prostate cancer, using a national cancer registry database (11). Besides the average causal effect, it is also of great interest to investigate whether there is TEH in this population for a more personalized treatment decision making (12). The detection of TEH, however, is complicated by right censoring of the survival time (e.g. due to death or loss-to-follow-up) as well as challenges in accurately modeling the complex adjusted survival curves in each group. To meet the methodological needs posed by these emerging epidemiological research questions, we investigate in this article the operating characteristics of three state-of-the-art ML and deep learning (DL) techniques, AFT-BART developed in Henderson et al. (13), random survival forests (RSF) introduced by Ishwaran et al. (14) and DeepSurv proposed by Katzman et al. (15) for estimating the ITE. We choose these three ML/DL techniques because they are specifically designed for right-censored survival data and different versions of these methods for continuous or binary outcomes have become increasingly popular in the causal inference literature (3, 4, 16, 17). We also compare these ML/DL methods with two commonly used regression methods, the AFT and Cox Proportional Hazards (PH) model. We estimate the ITE by directly modeling the outcome conditional on the potential confounders for both treatment and control groups and averaging the estimates using g-computation, which is equivalent to standardization in epidemiology (18). The outcome model will henceforth be referred to as the response surface model. We contribute sets of simulations representing complex causal inference settings with right-censored data, and evaluate the empirical performance of these ML/DL methods.

NOTATION AND METHODS

Individual survival treatment effect (ISTE)

Let Z_i be a binary treatment variable with 1 for treatment and 0 for control, and \mathbf{X}_i be a vector of measured confounders measured before treatment assignment. Let T_i denote the actual survival time and C_i the censoring time. The observed outcome consists of $Y_i = \min(T_i, C_i)$ and censoring indicator $\Delta_i = I(T_i < C_i)$. We proceed in the counterfactual outcome framework, and define the causal effect for individual i as a comparison of $T_i(1)$ and $T_i(0)$, representing the counterfactual survival times that would be observed under treatment and control, respectively. Throughout, we maintain the standard assumptions for drawing causal inference with observational studies (19):

- A1. Consistency: The observed outcome $T_i = Z_i T_i(1) + (1 - Z_i) T_i(0)$.
- A2. Positivity: the propensity score $e(\mathbf{X}_i) = P(Z_i = 1 | \mathbf{X}_i)$ is bounded away from 0 and 1.
- A3. Conditional exchangeability: $T_i(z) \perp\!\!\!\perp Z_i | \mathbf{X}_i$ for $Z_i = z, z \in \{0,1\}$.

We further assume that the counterfactual survival time is independent of the censoring time given the pre-treatment covariates and treatment, $T_i(z) \perp\!\!\!\perp C_i | \mathbf{X}_i, Z_i$, for $Z_i = z, z \in \{0,1\}$, which also implies $T_i \perp\!\!\!\perp C_i | \mathbf{X}_i, Z_i$. Following Chen and Tsiatis (20), we refer to this assumption as conditionally noninformative censoring.

For survival outcomes, we define the ITE based on the median survival time, which is a natural summary statistics of the entire survival curve and of clinical relevance (21). We refer to such an estimand as the individual survival treatment effect (ISTE). Given $\mathbf{X}_i = \mathbf{x}$, the ISTE for individual i is defined as,

$$\omega(\mathbf{x}) = E(\theta_i(1)^{0.5} - \theta_i(0)^{0.5} | \mathbf{X}_i = \mathbf{x}),$$

where $S(T_i(z) > \theta_i(z)^{0.5} | \mathbf{X}_i = \mathbf{x}) = S(T_i(z) \leq \theta_i(z)^{0.5} | \mathbf{X}_i = \mathbf{x}) = 0.5$ for $z \in \{0, 1\}$. Because only the outcome, $\{Y_i, \Delta_i\}$, corresponding to the actual treatment assignment is observed, the ISTE as a function of the unknown counterfactuals is not directly identifiable. However, under assumptions A1-A3, we have

$$\begin{aligned} & S(T(1) > t | Z = 1, \mathbf{X} = \mathbf{x}) - S(T(0) > t | Z = 0, \mathbf{X} = \mathbf{x}) \\ &= S(T > t | Z = 1, \mathbf{X} = \mathbf{x}) - S(T > t | Z = 0, \mathbf{X} = \mathbf{x}), \end{aligned}$$

which allows us to estimate $\omega(\mathbf{x})$ by fitting two survival regression models, \mathcal{M}_0 and \mathcal{M}_1 , to the observed data $\{f(\mathbf{X}_i, Y_i, \Delta_i) : Z_i = 0\}$ and $\{f(\mathbf{X}_i, Y_i, \Delta_i) : Z_i = 1\}$, respectively. To estimate ISTE, we predict for each data point two survival curves conditional on $\{X_i = \mathbf{x}, Z_i = z\}$, $\hat{S}_{\mathcal{M}_j}(t, \mathbf{x}, z)$, from model \mathcal{M}_j , $j = 0, 1$. The ISTE estimator is then defined as

$$\hat{\omega}(\mathbf{x}) = \hat{\theta}_{\mathcal{M}_1}^{0.5} - \hat{\theta}_{\mathcal{M}_0}^{0.5}, \quad (1)$$

where $\hat{S}_{\mathcal{M}_1}(\hat{\theta}_{\mathcal{M}_1}^{0.5}, \mathbf{x}, 1) = 0.5$ and $\hat{S}_{\mathcal{M}_0}(\hat{\theta}_{\mathcal{M}_0}^{0.5}, \mathbf{x}, 0) = 0.5$.

Models for estimating ISTE

We briefly introduce each method considered. Additional technical details about how to obtain the individual survival curves -- which represent an essential ingredient for estimating ISTE following equation (1) -- and software implementation are presented in the Supplementary Material.

AFT-BART

The AFT-BART model relates the failure time T to the covariates through

$$\log T = f(\mathbf{X}) + W,$$

where $f(\mathbf{X})$ is a sum-of-trees BART model and W is the residual term, which can be assumed to follow a normal distribution, resulting in a semi-parametric model; we term this model by AFT-BART-SP. Henderson et al. (13) model W as a location-mixture of Gaussian densities utilizing the centered Dirichlet process (CDP). This approach leads to a nonparametric model, which we refer to as AFT-BART-NP.

RSF

The RSF approach extends Breiman's RF to right-censored survival data (14). The key idea of the RSF algorithm is to grow a binary survival tree and construct the ensemble cumulative hazards function (CHF). Each terminal node of the survival tree contains the observed survival times and the 0-1 censoring information for individuals who fall in that terminal node. The out-of-bag (OOB) ensemble CHF can be used to compute the survival curves.

DeepSurv

DeepSurv is a recent Cox regression tool based on deep neural network (15). The input to the network is an individual's baseline covariates. The output of the network estimates the log-risk function in the Cox model. We then calculate the Nelson-Aalen (N-A) estimate of the baseline cumulative hazard using the estimated log-risk function and compute the individual survival curve by relating the survival function to the hazard function.

Parametric AFT

A parametric AFT model (22) proposes an explicit functional relationship between the covariates and the failure time T with an error term W , for which a variety of distributions can be assumed.

In our simulations, we assume a standard extreme value distribution and a normal distribution, for which the survival time has a Weibull distribution and a log-normal distribution, respectively.

Cox Proportional Hazards Model

A Cox proportional hazards (PH) model (23) assumes that the hazard ratio is constant across the lifespan. The parameter in the model can be estimated by maximizing the partial likelihood. We can obtain the N-A estimate of the baseline cumulative hazard and compute the individual survival curve.

SIMULATION

Design

We carry out a series of simulation studies to compare the above survival models for estimating the ISTE in the context of observational studies. Throughout we consider two levels of total sample size: $n = 500$ and $n = 5000$, representing small and large studies. We simulate $p = 10$ independent covariates, where covariates X_1, \dots, X_5 are drawn from the standard $N(0,1)$, and X_6, \dots, X_{10} from Bernoulli (0.5). The treatment assignment is generated from $Z \sim Bernoulli(e(\mathbf{X}))$, where

$$\text{logit}(e(\mathbf{X})) = \alpha_0 + \alpha_1 X_1 + \alpha_2 X_2 + \alpha_3 X_3 + \alpha_4 X_4 + \alpha_5 X_5 + \alpha_6 X_6 + \alpha_7 X_7 + \alpha_8 X_8 + \alpha_9 X_9 + \alpha_{10} X_{10},$$

and $(\alpha_1, \alpha_2, \alpha_3, \alpha_4, \alpha_5, \alpha_6, \alpha_7, \alpha_8) = (-0.1\psi, -0.9\psi, -0.3\psi, -0.1\psi, -0.2\psi, -0.4\psi, 0.5\psi)$. We chose $\psi = \{1, 2.5, 5\}$ to represent strong, medium and weak covariate overlap. The distribution of the true PS is shown in Figure 1. In particular, the degree of overlap determines the effective sample size for estimating population ATE (24), and we aim to explore the implication of

overlap for estimating ISTE. The intercept in the true PS model α_0 is chosen such that the proportion of treated remains approximately 0.5.

[Figure 1 about here]

We simulate the true potential survival times T from the Weibull survival curve,

$$S(t|X = \mathbf{x}, Z = z) = e^{-\{d_z \exp[m_z(\mathbf{x})]t\}^\eta}, \quad z \in \{0,1\}. \quad (2)$$

We consider the Weibull distribution as it has both the AFT and PH representations, and so could lead to scenarios where each one of these assumptions is valid. Using the inverse transform sampling, we generate nonparallel (potential) survival response surfaces, inducing confounded heterogenous treatment effect (CHTE) as follows,

$$T(z|\mathbf{X}) = \left\{ \frac{-\log U}{d_z \exp(m_z(\mathbf{X}))} \right\}^{1/\eta}, \quad z \in \{0, 1\},$$

where $U \sim \text{Unif}(0,1)$ is a random variable following a uniform distribution on the interval [0,1], $d_z = 1200$ for $z = 0$, and $d_z = 2000$ for $z = 1$, and η is the shape parameter that can induce nonproportional hazards (nPH). We consider three structures for $m_z(\mathbf{X})$, leading to three heterogeneous settings (HS) with CHTE of different complexities:

- (i) $m_1(\mathbf{X}) = -0.2 + 0.1/(1 + e^{-X_1}) - 0.8 \sin(X_3) - 0.1X_5^2 - 0.3X_6 - 0.2X_7$, and
 $m_0(\mathbf{X}) = 0.2 - 0.5X_1 - 0.8X_3 - 1.8X_5 - 0.9X_6 - 0.1X_7$
- (ii) $m_1(\mathbf{X}) = -0.2 + 0.1/(1 + e^{-X_1}) - 0.8 \sin(X_3) - 0.1X_5^2 - 0.3X_6 - 0.2X_7$, and
 $m_0(\mathbf{X}) = -0.1 + 0.1X_1^2 - 0.2 \sin(X_3) + 0.2/(1 + e^{-X_5}) + 0.2X_6 - 0.3X_7$
- (iii) $m_1(\mathbf{X}) = 0.5 - 0.1/(1 + e^{-X_2}) + 0.1 \sin(X_3) - 0.1X_4^2 + 0.2X_4 - 0.1X_5^2 - 0.3X_6$,
and $m_0(\mathbf{X}) = -0.1 + 0.1X_1^2 - 0.2 \sin(X_3) + 0.2/(1 + e^{-X_5}) + 0.2X_6 - 0.3X_7$

Across all three outcome generating processes, X_1, X_3, X_5, X_6, X_7 are confounders that predict both the treatment assignment and the outcome. In scenario (i), there is a nonlinear covariate

effect only in the treated group. In scenario (ii), the nonlinear covariate effects are present in both treatment groups. Scenario (iii) is similar to scenario (ii) except that a non-overlapping set of covariates are included in the treated and control groups; this additional complexity represents an additional source of TEH. Finally, when simulating the potential survival times, the parameter η is set to be 2 to satisfy the PH assumption. To induce nPH, η is set to be $e^{0.7-1.8X_3+0.8X_7}$ for $Z = 0$, and $e^{0.9-0.5X_1+0.5X_2}$ for $Z = 1$. Throughout, we generate the censoring time C independently from an exponential distribution with rate parameters 0.007 and 0.02, corresponding to two levels of censoring rate (CR), 20% and 60%. The Kaplan-Meier curves of the simulated survival data are displayed in Figure S1 of Supplemental Materials. R code to reproduce our simulations is available on GitHub.

Performance Measures

We first assess the overall precision in the estimation of heterogenous effects (PEHE) (4) for each method considered using

$$\sqrt{\frac{1}{n} \sum_{i=1}^n [\hat{\omega}_i(\mathbf{X}_i) - E(\theta_i(1)^{0.5} - \theta_i(0)^{0.5} | \mathbf{X}_i = \mathbf{x})]^2},$$

where $E(\theta_i(1)^{0.5} - \theta_i(0)^{0.5} | \mathbf{X}_i = \mathbf{x})$ is the difference between two potential median survival times calculated from each simulation sample, and $\hat{\omega}_i(\mathbf{X}_i)$ is the estimated ISTE for individual i . A smaller value of PEHE indicates better accuracy and is considerable favorable. For computational considerations, we replicate each of our simulations independently $B = 250$ times for $n = 5000$ and $B = 1000$ times for $n = 500$. We summarize the mean and standard deviation (SD) of the PEHE across B replications.

To further evaluate the operating characteristics of each method in recovering the within subgroups, we subclassify the individuals into $\mathcal{G} = \{\mathcal{G}_1, \dots, \mathcal{G}_K\}$ based on K quantiles of the true PS, $e(\mathbf{X})$, and calculate relative bias and root mean squared error (RMSE) for each method. By investigating the performance of each method in distinct covariate regions with different proportions of treatment assignment, we can assess the robustness of each method to data sparsity. Given an estimator $\hat{\omega}$ of ω , the bias for group \mathcal{G}_k is defined as

$$\text{Bias}(k) = E(\hat{\omega}(\mathbf{X}) | \mathbf{X} \in \mathcal{G}_k) - E(\omega(\mathbf{X}) | \mathbf{X} \in \mathcal{G}_k), \quad k = 1, \dots, K.$$

where $\hat{\omega}(\mathbf{X})$ is the estimated ISTE averaged over all individuals in \mathcal{G}_k , and $\omega_{k,b}$ is the true average ISTE. Similarly, we define the RMSE of $\hat{\omega}$ among subgroup \mathcal{G}_k as

$$\text{RMSE}(k) = \sqrt{E[(\hat{\omega}(\mathbf{X}) - \omega(\mathbf{X}))^2 | \mathbf{X} \in \mathcal{G}_k]}, \quad k = 1, \dots, K.$$

For each individual in subgroup \mathcal{G}_k , we compute the true ISTE $\omega(\mathbf{x})$ as the difference in the median survival times of two potential Kaplan-Meier survival curves of individuals in \mathcal{G}_k ; and estimate the ISTE $\hat{\omega}(\mathbf{X})$ by differencing the predicted pair of counterfactual median survival times of the potential individual survival curves. Let $\mathcal{G}_{k,b}$ contain individuals within the q_k quantile of the PS from replication b , and $N_{\mathcal{G}_{k,b}}$ denote its size. Let ω and $\hat{\omega}_b$ be the true ISTE and ISTE estimator from replication b , respectively. The relative bias is estimated by

$$\widehat{\text{RelBias}}(k) = \frac{1}{B} \sum_{b=1}^B (\hat{\omega}_{k,b} - \omega_{k,b}) / \omega_{k,b},$$

where $\hat{\omega}_{k,b} = \frac{1}{N_{\mathcal{G}_{k,b}}} \sum_{\{\mathbf{X}: \mathbf{X} \in \mathcal{G}_{k,b}\}} \hat{\omega}_b(\mathbf{X})$ and $\omega_{k,b} = \frac{1}{N_{\mathcal{G}_{k,b}}} \sum_{\{\mathbf{X}: \mathbf{X} \in \mathcal{G}_{k,b}\}} \hat{\omega}_b(\mathbf{X})$. The RMSE is estimated using

$$\widehat{\text{RMSE}}(k) = \frac{1}{B} \sum_{b=1}^B \frac{1}{N_{\mathcal{G}_{k,b}}} \sum_{\{\mathbf{X}: \mathbf{X} \in \mathcal{G}_{k,b}\}} [\hat{\omega}_b(\mathbf{X}) - \omega_b(\mathbf{X})]^2.$$

Finally, while it is generally challenging to obtain valid confidence intervals for the estimates of survival causal effects using frequentist ML/DL methods, the Bayesian methods naturally produce coherent posterior credible intervals. For this reason, we additionally summarize the empirical coverage probability (CP) for the winner of the two AFT-BART methods.

RESULTS

PEHE, Relative Bias and RMSE Under Strong Overlap

We first consider the performance of each method without the challenge due to lack of overlap. Table 1 summarizes, for sample size $n = 5000$, the mean and SD of PEHE under each simulation configuration with strong covariate overlap (see Panel A in Figure 1). First, all ML/DL methods yield significantly smaller PEHE than AFT and Cox PH models across all simulation scenarios. Second, as the heterogeneity setting becomes more complex, ML/DL methods tend to have better performance by having smaller PEHE. In comparison, (semi) parametric methods tend to perform worse. All methods show less precision in estimating ISTE under nPH and a larger censoring rate. Third, among the four machine/deep learning approaches, AFT-BART-NP has the best performance across all simulation configurations. Table S1 in the Supplemental Materials displays PEHE for $n = 500$. The findings are qualitatively similar except that the PEHE becomes larger with a smaller sample size.

[Table 1 about here]

The relative bias and RMSE results within subgroups defined by quantiles of the true PS are summarized in Figure S2-S5 in the Supplemental Materials. The traditional AFT and Cox PH models have substantially larger bias and RMSE compared to ML/DL methods across all

scenarios; and when the underlying assumptions are violated, these methods led to worse results. Specifically, the Cox PH has the largest relative bias and RMSE under the nPH setting and AFT-Lognormal has the largest relative bias and RMSE when the true outcomes are simulated from the Weibull curves. Among the ML/DL methods, AFT-BART-NP generally maintained the best performance, and even more so with a large sample size is large and the PH. The advantage of AFT-BART-NP over the other three approaches, however, is moderate. Overall, the tightness of the range of relative bias values for ML/DL methods under the most complex HS (iii) when $n = 5000$ demonstrate their substantially superior performance over the traditional parametric implementations.

Impact of Covariate Overlap

When there is strong covariate overlap, AFT-BART-NP demonstrates moderately better performance than AFT-BART-SP, RSF and DeepSurv. As the degree of covariate overlap decreases, the advantage of AFT-BART-NP becomes more apparent. Figure 2 shows that for the most challenging scenario (HS (iii) + nPH + 60% censoring), both the relative bias and RMSE increase as the lack of overlap increases for all ML/DL method and for both sample sizes. However, AFT-BART-NP appears to be the most robust approach with the median relative bias around 5% in the most extreme scenario ($\psi = 5$); DeepSurv appears to have the largest increase in both relative bias and RMSE as the degree of overlap decreases.

[Figure 2 about here]

Overall Performance

In Figure 3, we provide an overall assessment of the methods across the simulation scenarios.

(10) Specifically, in each of the B simulation iterations, we compute the percent increase in PEHE with respect to the best performer for this iteration. The percent increase in PEHE of method i with respect to the best is given by $(\text{PEHE}_i/\text{PEHE}_{\min} - 1) \times 100$. For a given iteration, only the best method will correspond to a percent increase of exact zero while the others lead to positive values. Figure 3 presents the boxplots of percent increase in PEHE over all 3500 (simulations for $n = 5000$ and 14000 simulations for $n = 500$ (see Figure legend for more details). Evidently, the AFT-BART-NP method outperformed the other approaches for having the smallest median and mean percent increase in PEHE; the advantage is more pronounced for a larger sample size $n = 5000$.

[Figure 3 about here]

Coverage Probability

An additional advantage of AFT-BART-NP is that it naturally produces coherent posterior intervals in contrast to other ML/DL methods such as RSF and DeepSurv, for which it is unclear how to derive simple and valid interval estimates for heterogeneous survival causal effects. Table 2 provides CPs of the AFT-BART-NP estimators of the survival causal effect for subgroups defined by the true PS quantiles, under HS (iii), 60% censoring rate and different degrees of covariate overlap. In this most challenging CHTE scenario, when there is strong or medium level of overlap, AFT-BART-NP generally provides close-to-nominal CP across all subgroups for both sample sizes without respect to whether the PH assumption is satisfied. Furthermore, under weak overlap for which it is challenging to correctly estimate the traditional average causal effects (24), the AFT-BART-NP approach could still provide nominal CP among the data region

where treatment assignment is balanced (e.g., the 25th subgroup). However, the CP decreases as we move towards the tail regions of the PS distribution, echoing the previous findings for estimating the population ATE. A full summary of CPs across different scenarios is visualized in Figure S of Supplemental Materials and leads to the same conclusion.

[Table 2 about here]

DISCUSSION

Traditional detection of TEH has been carried out by first identifying effect modifiers by subject matter experts and then estimating the treatment effect within each subgroup. In observational data with complex heterogeneity of treatment effect, this *a priori* specification that separates the issues of confounding and TEH becomes infeasible, especially with a large number of pre-treatment covariates. Relying on the counterfactual outcome framework, flexibly modeling of the response outcome is well-suited for the estimation of TEH. However, ongoing discussions about causal methods for estimating TEH in observation data have largely focused on non-survival data. For example, tree-based methods such as BART and RF have recently emerged as popular approaches to causal effect estimation for continuous or binary outcomes. On the other hand, DeepSurv was shown to be a state-of-the-art deep neural network method within the framework of Cox regression for modeling interactions between an individual's covariates and treatment effectiveness. We adapt these three modern ML/DL outcome modeling tools for estimating ISTE and provide new empirical evidence using simulations representative of complex confounding and heterogeneity settings with censored survival data.

All ML/DL methods significantly outperform the traditional AFT and Cox PH models in estimating TEH across our simulation scenarios. Among the four ML/DL methods considered, the nonparametric version of the AFT-BART model generally outperformed the competing approaches. The advantage of AFT-BART-NP becomes more pronounced with a larger sample size and in a more complex CHTE setting. On the other hand, AFT-BART-NP is also the only ML method that enables full posterior inference including credible interval estimates for ISTE and subgroup average causal effect. In particular, when there is strong or moderate overlap, AFT-BART-NP could provide close-to-nominal CP for almost all average causal effect among subgroups defined by the true PS. Under lack of overlap, AFT-BART-NP still provides close-to-nominal CP for the subgroup near the centroid of the PS distribution, where the treatment assignment is relatively balanced. As previous simulations for TEH rarely considered the lack of overlap, our results offer new insights. Importantly, findings for the lack of overlap setting demonstrate that even though estimating ISTE becomes challenging at the tails of the PS distribution due to data sparsity, estimating ISTE among the centroid of the PS distribution remains both feasible and accurate. In fact, the centroid region represents the individuals at clinical equipoise and are similar to the overlap population resembling those in a randomized trial (24). Finally, because the AFT-BART-NP is comparable to RSF and DeepSurv in terms of computational efficiency, it may be preferred for providing valid inference without more extensive computations.

In general, the g -computation represents a simple and powerful approach for causal effect estimation, with the caveat that accurate estimation critically depends on correct specification of the response surface model. With the advancement of machine learning techniques, more precise

modeling of the response surface can be achieved, which can naturally serve as the building block for more individualized estimation. The ISTE estimates can then be utilized to explore the degree of TEH. As in the second stage of the virtual twins approach, the ISTE estimates could be used as the outcome and a tree diagram could be fitted to identify predictors that explain differences in the ISTE and the characteristics of each subgroup. In Lu et al. (3), the ISTE estimates are used as the dependent variable in a standard regression model to explain between-subgroup differences in treatment effect. As suggested in Anoke et al (5), averaging ISTE estimates within a pre-specified subgroup (e.g., Female vs. Male) can also facilitate the exploration of the TEH. Given these existing tools, the ISTE from a flexible response surface model can yield insights not only for the population ATE but also for the detection of TEH.

There are several limitations of our simulation study. First, we a priori defined subgroups based on the PS, so that we could compare the operating characteristics of each method in estimating the ISTE on the same basis. Future work is required to explore strategies to estimate the number of underlying subgroups from the data. Second, our simulations were aimed at providing new empirical evidence about the operating characteristics of state-of-the-art ML/DL techniques for estimating TEH, and only provided coverage probability for AFT-BART-NP. Although the Bayesian machine learning method AFT-BART could naturally provide coherent posterior intervals for the target estimand, it is generally challenging to estimate the valid variance of the median survival time using DeepSurv and RSF, without resorting to more computationally intensive sample-splitting methods (2, 25-27). Developing and investigating new methods for the variance and interval estimation for DeepSurv and RSF represent an important avenue for future research. Finally, as in all causal inference work with observational data, we require an

untestable assumption that the pre-treatment covariates are sufficient to de-confound the relationship between treatment and outcome. In practice when this assumption is questionable, developing ML/DL-based sensitivity analyses to capture the effects of unmeasured confounding for estimating TEH would be a worthwhile and important contribution.

Reference

1. Foster JC, Taylor JM, Ruberg SJ. Subgroup identification from randomized clinical trial data. *Statistics in Medicine* 2011;30(24):2867-80.
2. Wager S, Athey S. Estimation and Inference of Heterogeneous Treatment Effects using Random Forests. *Journal of the American Statistical Association* 2018;113(523):1228-42.
3. Lu M, Sadiq S, Feaster DJ, et al. Estimating Individual Treatment Effect in Observational Data Using Random Forest Methods. *Journal of Computational and Graphical Statistics* 2018;27(1):209-19.
4. Hill JL. Bayesian Nonparametric Modeling for Causal Inference. *Journal of Computational and Graphical Statistics* 2011;20(1):217-40.
5. Anoke SC, Normand S-L, Zigler CM. Approaches to treatment effect heterogeneity in the presence of confounding. *Statistics in Medicine* 2019;38(15):2797-815.
6. Henderson NC, Louis TA, Rosner GL, et al. Individualized treatment effects with censored data via fully nonparametric Bayesian accelerated failure time models. *Biostatistics* 2020;21(1):50-68.
7. Tian L, Alizadeh AA, Gentles AJ, et al. A Simple Method for Estimating Interactions Between a Treatment and a Large Number of Covariates. *Journal of the American Statistical Association* 2014;109(508):1517-32.
8. Shen J, Wang L, Daignault S, et al. Estimating the Optimal Personalized Treatment Strategy Based on Selected Variables to Prolong Survival via Random Survival Forest with Weighted Bootstrap. *Journal of Biopharmaceutical Statistics* 2018;28(2):362-81.
9. Cui Y, Kosorok MR, Wager S, et al. Estimating heterogeneous treatment effects with right-censored data via causal survival forests [electronic article]. *arXiv e-prints*. Advance Access: January 01, 2020.
10. Tabib S, Larocque D. Non-parametric individual treatment effect estimation for survival data with random forests. *Bioinformatics* 2019;36(2):629-36.
11. Ennis RD, Hu L, Ryemon SN, et al. Brachytherapy-Based Radiotherapy and Radical Prostatectomy Are Associated With Similar Survival in High-Risk Localized Prostate Cancer. *Journal of Clinical Oncology* 2018;36(12):1192-8.
12. Chen RC. Challenges of Interpreting Registry Data in Prostate Cancer: Interpreting Retrospective Results Along With or in Absence of Clinical Trial Data. *Journal of Clinical Oncology* 2018;36(12):1181-3.
13. Henderson NC, Louis TA, Rosner GL, et al. Individualized treatment effects with censored data via fully nonparametric Bayesian accelerated failure time models. *Biostatistics* 2018;21(1):50-68.
14. Ishwaran H, Kogalur UB, Blackstone EH, et al. Random survival forests. *Annals of Applied Statistics* 2008;2(3):841-60.

15. Katzman JL, Shaham U, Cloninger A, et al. DeepSurv: personalized treatment recommender system using a Cox proportional hazards deep neural network. *BMC Medical Research Methodology* 2018;18(1):24.
16. Hu L, Gu C, Lopez M, et al. Estimation of causal effects of multiple treatments in observational studies with a binary outcome. *Statistical Methods in Medical Research* 2020:0962280220921909.
17. Narendra T, Sankaran A, Vijaykeerthy D, et al. Explaining Deep Learning Models using Causal Inference [electronic article]. *arXiv e-prints*. Advance Access: November 01, 2018.
18. Robins J. A new approach to causal inference in mortality studies with a sustained exposure period—application to control of the healthy worker survivor effect. *Mathematical Modelling* 1986;7(9):1393-512.
19. Hernán MA, Robins JM. *Causal Inference: What If*. Boca Raton, FL: CRC Press; 2020.
20. Chen PY, Tsiatis AA. Causal inference on the difference of the restricted mean lifetime between two groups. *Biometrics* 2001;57(4):1030-8.
21. Mao H, Li L, Yang W, et al. On the propensity score weighting analysis with survival outcome: Estimands, estimation, and inference. *Statistics in Medicine* 2018;37(26):3745-63.
22. Kalbfleisch JD, Prentice RL. *The Statistical Analysis of Failure Time Data*. 2nd ed. Hoboken, NJ: Wiley Series in Probability and Statistics; 2002.
23. Cox DR. Regression Models and Life-Tables. *Journal of the Royal Statistical Society Series B (Methodological)* 1972;34(2):187-220.
24. Li F, Thomas LE, Li F. Addressing Extreme Propensity Scores via the Overlap Weights. *Am J Epidemiol* 2018;188(1):250-7.
25. Yifan Cui MRK, Stefan Wager, Ruoqing Zhu. Estimating heterogeneous treatment effects with right-censored data via causal survival forests. *arXiv e-prints* 2020:arXiv:2001.09887.
26. Díaz I. Machine learning in the estimation of causal effects: targeted minimum loss-based estimation and double/debiased machine learning. *Biostatistics* 2020;21(2):353-8.
27. Chernozhukov V, Chetverikov D, Demirer M, et al. Double/debiased machine learning for treatment and structural parameters. *The Econometrics Journal* 2018;21(1):C1-C68.

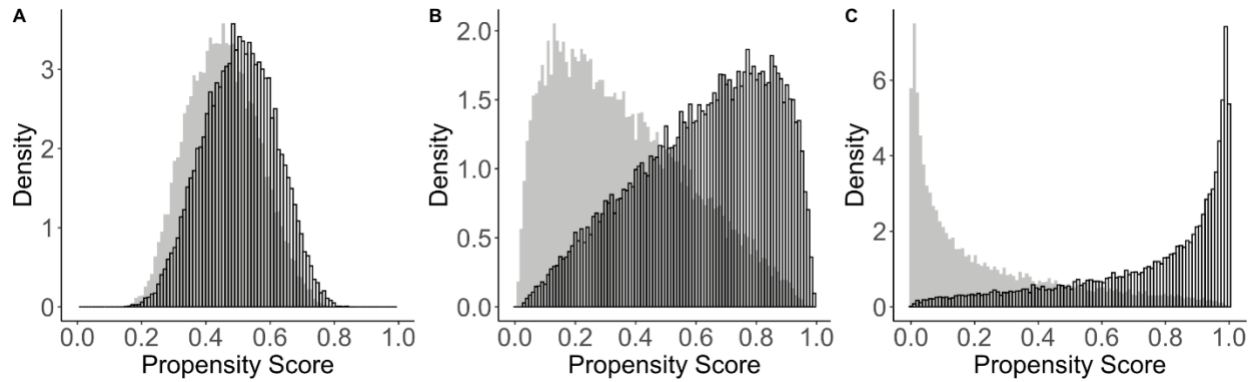


Figure 1. Distributions of PS generated from three treatment assignment mechanisms with an overall treatment prevalence equal to 0.5. The unshaded bars indicate the treated group; the gray shaded bars indicate the control group. Panels A–C show the distributions of PS corresponding to $\psi = 1$, $\psi = 2.5$, and $\psi = 5$, respectively.

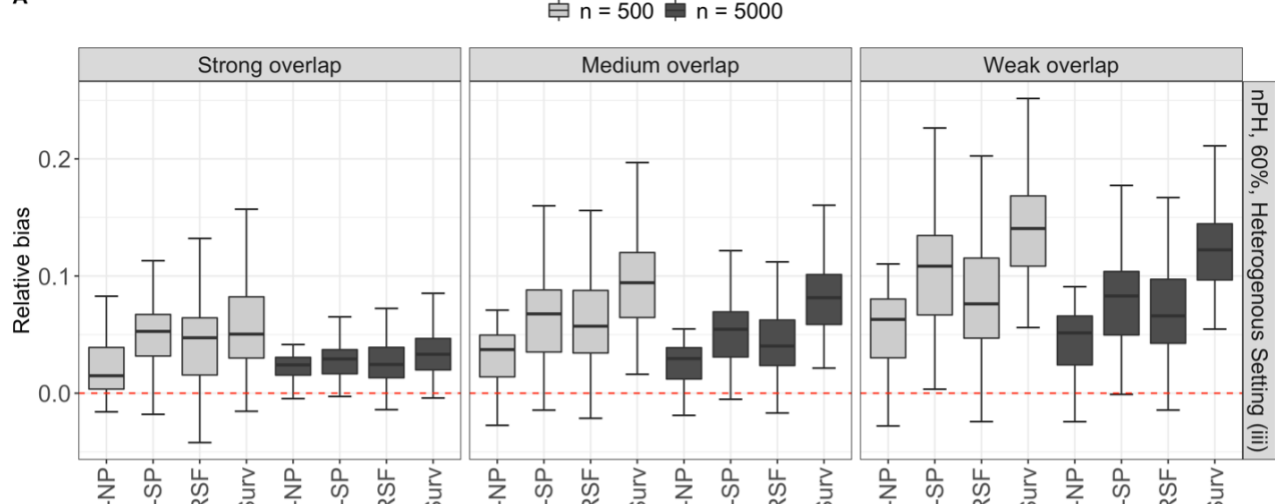
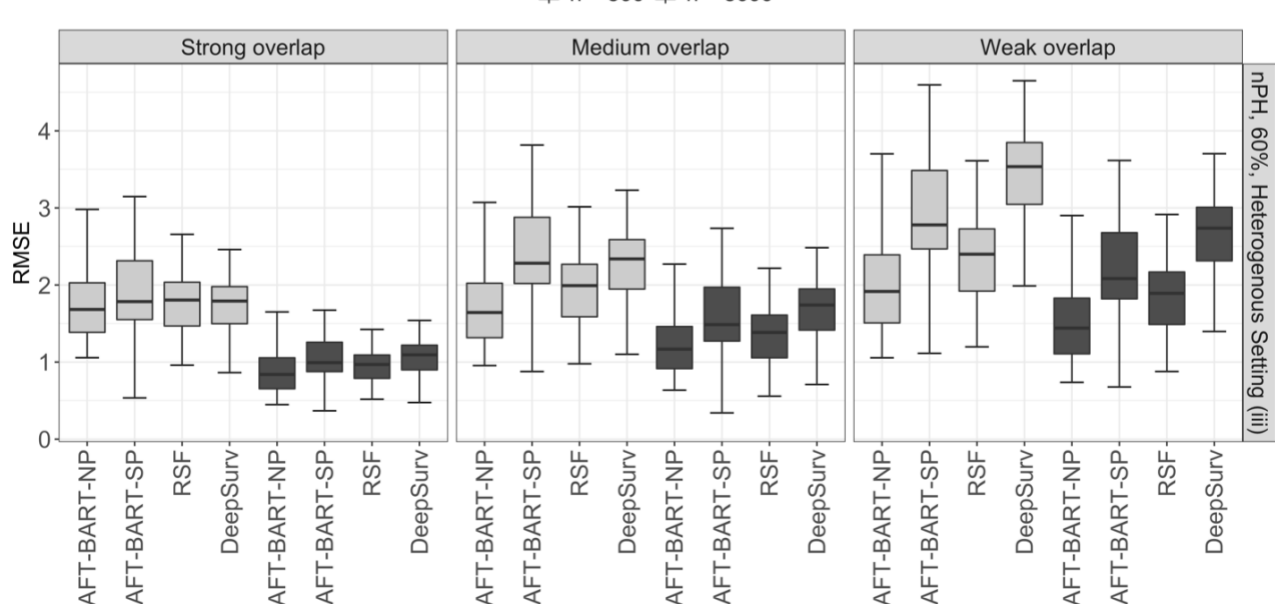
A**B**

Figure 2: Relative bias (Panel A) and RMSE (Panel B) results for each of four ML/DL methods and for strong, medium and weak covariate overlap.

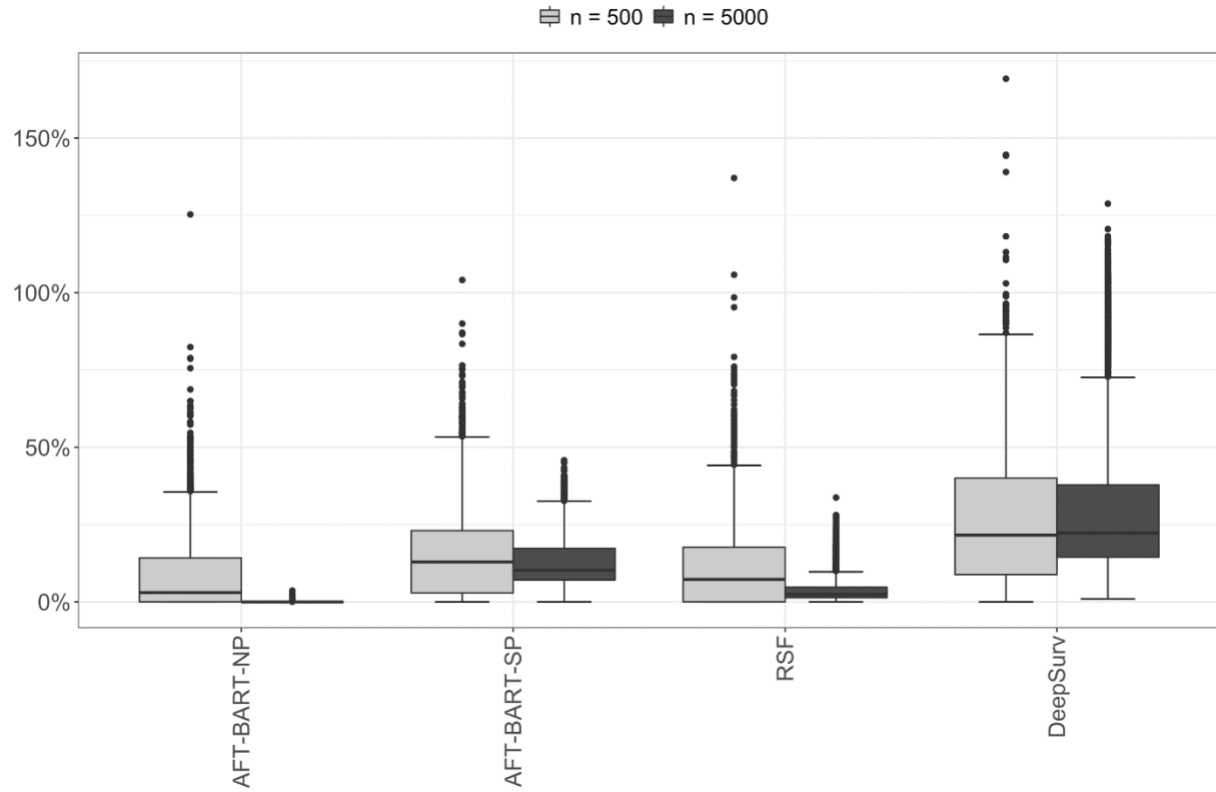


Figure 3. Comparison of ML/DL methods across all simulation configurations. The boxplots represent the distribution of the percent increase in PEHE with respect to the best performer for each simulation run for all runs. Smaller values are better. The total number of simulation runs for each boxplot equals to the number of scenarios multiplied by B ($B = 250, 1000$ for $n = 5000, 500$, respectively). There are 14 scenarios considered, as defined by 2 PH assumptions \times 2 censoring proportions \times 3 heterogenous settings with strong overlap + (medium overlap + weak overlap) \times 1 scenario (the most challenging one) with nPH, 60% censoring and HS (iii).

Table 1. Mean (SD) of PEHE for each method and each simulation configuration for $n = 5000$.

$E[\omega(x)]$ is true average treatment effect based on median survival time (in months).

		PH			nPH		
		HS(i)	HS (ii)	HS (iii)	HS(i)	HS (ii)	HS (iii)
$E[\omega(x)]$		14.03	14.58	13.09	13.59	13.89	12.01
CR = 20%	AFT-Lognormal	3.63 (0.14)	4.17 (0.15)	4.13 (0.14)	3.79 (0.13)	4.35 (0.16)	4.41 (0.17)
	AFT-Weibull	2.11 (0.12)	2.58 (0.12)	2.65 (0.12)	2.31 (0.13)	2.84 (0.13)	2.81 (0.13)
	Cox PH	2.16 (0.11)	2.61 (0.12)	2.61 (0.13)	3.81 (0.13)	4.38 (0.14)	4.39 (0.13)
	AFT-BART-NP	0.51 (0.03)	0.21 (0.02)	0.12 (0.02)	0.72 (0.07)	0.41 (0.04)	0.33 (0.04)
	AFT-BART-SP	0.56 (0.04)	0.24 (0.03)	0.15 (0.02)	0.78 (0.08)	0.44 (0.05)	0.36 (0.04)
	RSFs	0.53 (0.03)	0.22 (0.02)	0.13 (0.02)	0.73 (0.07)	0.42 (0.04)	0.33 (0.04)
	DeepSurv	0.62 (0.04)	0.29 (0.03)	0.22 (0.03)	0.82 (0.08)	0.47 (0.06)	0.41 (0.05)
		PH			nPH		
		HS(i)	HS (ii)	HS (iii)	HS(i)	HS (ii)	HS (iii)
$E[\omega(x)]$		15.64	16.13	13.02	13.92	14.32	12.23
CR = 60%	AFT-Lognormal	4.14 (0.14)	4.57 (0.15)	4.45 (0.15)	4.39 (0.18)	4.89 (0.19)	4.91 (0.18)
	AFT-Weibull	2.62 (0.12)	3.22 (0.13)	3.14 (0.13)	2.89 (0.16)	3.71 (0.14)	3.72 (0.13)
	Cox PH	2.63 (0.12)	3.21 (0.13)	3.22 (0.13)	4.41 (0.18)	4.83 (0.18)	4.83 (0.18)
	AFT-BART-NP	0.81 (0.04)	0.31 (0.04)	0.21 (0.02)	0.99 (0.09)	0.51 (0.06)	0.41 (0.04)
	AFT-BART-SP	0.84 (0.04)	0.34 (0.04)	0.24 (0.02)	1.04 (0.09)	0.56 (0.06)	0.45 (0.04)
	RSFs	0.82 (0.05)	0.32 (0.05)	0.22 (0.02)	1.01 (0.09)	0.52 (0.06)	0.41 (0.04)
	DeepSurv	0.85 (0.04)	0.38 (0.04)	0.26 (0.03)	1.09 (0.11)	0.59 (0.07)	0.51 (0.05)

Table 2. Coverage probability of AFT-BART-NP for 5 subgroups, defined by quantiles of true PS, for each of two sample sizes, PH and nPH, and for strong, medium and weak overlap, in the scenario of HS (iii) and 60% censoring. $\mathcal{G}_k = 1$ and $\mathcal{G}_k = 50$ have the most extreme PS, with the smallest values in $\mathcal{G}_k = 1$ and largest in $\mathcal{G}_k = 50$.

		Overlap			
		\mathcal{G}_k	Strong	Medium	Weak
nPH	$n = 5000$	1	0.95	0.91	0.53
		12	0.95	0.92	0.72
		25	0.96	0.95	0.94
		37	0.94	0.93	0.73
		50	0.95	0.91	0.52
	$n = 500$	1	0.96	0.89	0.55
		12	0.93	0.92	0.71
		25	0.95	0.94	0.94
		37	0.90	0.91	0.70
		50	0.95	0.89	0.52
PH	$n = 5000$	1	0.97	0.93	0.52
		12	0.94	0.94	0.73
		25	0.97	0.96	0.94
		37	0.95	0.93	0.71
		50	0.95	0.91	0.52
	$n = 500$	1	0.97	0.90	0.55
		12	0.96	0.92	0.70
		25	0.97	0.96	0.94
		37	0.94	0.93	0.69
		50	0.95	0.89	0.52